Hindawi
Science and Technology of Nuclear Installations
Volume 2019, Article ID 9273503, 16 pages
https://doi.org/10.1155/2019/9273503

Research Article

Engineering Design of a Mechanical Decladder for Spent Nuclear Rod-Cuts

Young-Hwan Kim, Yung-Zun Cho, Young-Soon Lee, and Jin-Mok Hur

Korea Atomic Energy Research Institute, Daedeok-daero 989-111, Yuseong-gu, Daejeon 305-353, Republic of Korea

Correspondence should be addressed to Young-Hwan Kim; yhkim3@kaeri.re.kr

Received 1 April 2019; Accepted 22 July 2019; Published 14 August 2019

Academic Editor: Michael I. Ojovan

A practical scale mechanical decladder that can slit spent nuclear fuel rod-cuts (hulls + pellets) of several tens of kg HM/batch is being developed to supply UO_2 pellets to a voloxidation process. The mechanical decladder is an apparatus for separating and recovering fuel material and cladding tubes by horizontally slitting the cladding tube of a fuel rod and a defective irradiated fuel rod. In this study, we address the engineering design of the mechanical decladder for the pretesting of rod-cut slitting. To obtain the requirements of the mechanical decladder, we first manufactured a slitter for testing based on the decladding and shearing conditions of hulls and pellets. The performance test of the testing device for decladding was carried out using a 2-CUT blade module and a 3-CUT blade module. We evaluated the decladding methods for the mechanical decladder and selected the 3-CUT blade module based on the results. A buckling measurement instrument was used to perform a buckling verification test according to the length of a rod-cut and to determine decladder dimensions. The optimum decladding rod-cut length for buckling prevention was calculated. Furthermore, we analyzed the decladding mechanism for various slitting methods. Design/fabrication and preliminary tests of the practical scale mechanical decladder were also performed. For this purpose, we constructed the main mechanism by utilizing the SolidWorks modeling and analysis program and fabricated a new mechanical decladder. Based on the derived requirements, a mechanical decladder with three main modules was designed and fabricated for testing. Simulated rod-cuts of zircaloy were also manufactured to test the basic performance of the decladder, and a data acquisition system was constructed using RSC 232 to measure decladding force and velocity. In the basic test, the rod-cut was completely sectioned into three evenly spaced locations by the new mechanical decladder.

1. Introduction

Spent fuel, which is the essential by-product of electricity generation by nuclear power reactors, is a highly radioactive waste. However, it could be a valuable asset if it is effectively recycled. As the cumulative amount of spent fuel is increasing in Korea, the development of methods for the reliable and effective management of this spent fuel has become an important mission for the Korea Atomic Energy Research Institute (KAERI). Considerable research and development effort is being made to develop a management technology that will enhance environmental friendliness and proliferation resistance and maximize the use of available energy resources [1, 2]. Based on this, the KAERI is developing a mechanical head-end process for pyroprocessing. The mechanical head-end processing of spent fuel (SF) disassembly, extraction of rods, shearing of the extracted rods, and mechanical decladding are performed in advance as the head-end process of the pyroelectroreduction process. A mechanical decladding device for rod-cuts is necessary for the oxidation processing of spent fuel in the head-end process [3, 4]. The recovery of fuel materials in cladding tubes is extremely important for the recycling of spent nuclear fuel. A mechanical decladding method and an oxidative decladding method are commonly used for the recovery of fuel materials [5, 6]. However, at the KAERI, a slitting technology for mechanical decladding methods is used for recovering fuel materials in the form of fuel particles by slitting cladding tubes. The KAERI has developed a longitudinal slitter concept for preliminary testing and a

mechanical decladder that can handle several tens of kg HM/batch to supply UO_2 fragments to a voloxidation process [7, 8]. This concept consists of multiple rows of cutting wheels that are evenly spaced at 120° intervals around the circumference of a fuel pin. The rows of cutting wheels are indexed from the center of a cutting assembly to progressively cut into tubing [9]. Upon exiting the cutting assembly, tubing sections can be forced against simulated pellets to splay hulls outward while allowing contents to be collected directly below the assembly. This device design is based on the triaxial slitter design [10]. The mechanical decladder works as follows: a cutting rod of spent nuclear fuel is placed at the entrance of a module, and subsequently, it is inserted into the center of the module by an extrusion pin. The cutting rod then passes through the module and is simultaneously separated into several pieces by the blades inside the module. The pieces of the pellets in the fuel rod are then recovered. In this study, we focused on the engineering design of a mechanical decladder that can slit several tens of kg HM/batch. The study consists of five parts, specifically blade module test, buckling test, mechanism analysis, decladder design, and basic performance tests. Blade module pretesting is conducted by employing a prototype device to obtain design conditions. Buckling testing is performed using a buckling machine and an indicator to determine the optimum rod-cut length. We consider driving methods and various slitting mechanisms, such as vertical, horizontal, and slant types, to obtain the optimum mechanical decladding method. The main mechanism is designed and constructed by utilizing the SolidWorks modeling and analysis program. Finally, the simulated rod-cuts of zircaloy are used for the performance evaluation of the mechanical decladder. The design data of the new mechanical decladder will be utilized in the design of a more efficient decladder in the future.

2. Decladding Design Requirements

2.1. Head-End Process. Figure 1 shows a flow chart of the head-end process, which is one of the key pyroprocessing technologies for treating spent oxide fuel. This technology has been making considerable progress since it was proposed in the late 1990s by the KAERI. The main objectives of pyroprocessing are to reduce the heat load, radioactivity, and volume of processed spent fuel by removing heat-generating elements and transforming oxide fuel into metal fuel for disposal and/or recycling [11]. The head-end process consists of three main processes: mechanical decladding, voloxidation, and compaction [12]. After disassembly processing, in mechanical decladding, an extrusion pin transfers force to the blade modules in a blade module housing through a hydraulic cylinder. A load cell and the extrusion pin are operated on a loading unit. The loading unit measures decladding force when rods are penetrated and slit. The length of the part of the simulated rods and pin at the point where they pass through the cutting module is set to a minimum of approximately 500 mm. After decladding, UO_2 fragments are transferred to the voloxidation process. In this process, pellet-type SFs are pulverized via oxidation under an air-blowing condition and certain volatile fission products are removed from the produced powders using air flow [10]. Then, U_3O_8 powders are moved to the compaction process for U_3O_8 pellets, and the produced powders are introduced into a compactor. The recovery efficiency of the compaction process depends on the extent of separation of the U_3O_8 powders from hulls.

As shown in Figure 2, we consider five processes for designing a mechanical decladder: blade module test, buckling test, mechanical analysis for design requirements, decladder design, and performance test for verification.

2.2. Mechanical Decladding. A mechanical decladding technology for slitting rod-cuts is required to enhance the oxide reduction treatment of spent fuel. The mechanical decladder is an apparatus for separating and recovering fuel material and cladding tubes by horizontally slitting the cladding tube of a fuel rod and a defective irradiated fuel rod.

The cladding tubes of fuel rods are manufactured in a variety of sizes, such as a length of several meters, an outer diameter of several millimeters to tens of millimeters, and a thickness of approximately one millimeter or less. The oxidative decladding method requires fuel rods to be cut into extremely short lengths such as tens of millimeters. In contrast, the mechanical decladding method requires fuel rods to be cut into various lengths and thicknesses according to an applied scheme. Moreover, the mechanical decladding technology can slit all kinds of rod-cuts by employing 3-CUT modules of various sizes.

Blade modules were considered to enhance mechanical decladding technology. The decladding of fuel rods was performed by rotating three circular cutting blades inserted among rollers arranged at 120° intervals. The cutting blades were rotated via the extrusion of fuel rods from multiple rollers. The force for cutting the fuel rods was adjusted by controlling steel plates [13]. The forces applied to the rollers were generated by a hydraulic cylinder, and hydraulic pressure was controlled by a hydraulic pressure controller.

2.3. Blade Module Test. Decladding requirements were derived by the decladding test of a prototype device according to the slope of the blade modules. For the design of the device, the decladding conditions of pellets and hulls were checked and the cutting force requirements of the cutting blades were considered. Based on this, a tool to test simulated rods and cutting force was produced. Additionally, we used a Zry-4 tube with aluminum pellets instead of spent fuel tubes with high toxicity as simulated pellets. The tube was punched at both ends and fixed to prevent fragments from running out of the tube. The major requirements were assumed to be a throughput of 50 kg·HM/day and 250 working days (full capacity) per year. Based on the KSFA type (16×16), the decladder design was conditioned to process 10 tons·of HM/year fuel with 85% availability.

To design the mechanical decladder, we first manufactured a slitter for testing based on the decladding and shearing conditions of hulls and pellets. The configuration and functions of the test apparatus are described below.

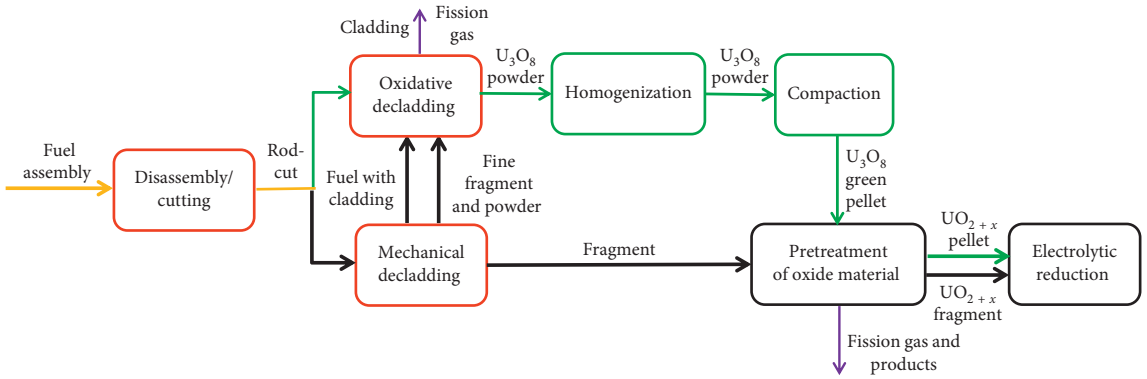

Figure 1: Entire head-end process.

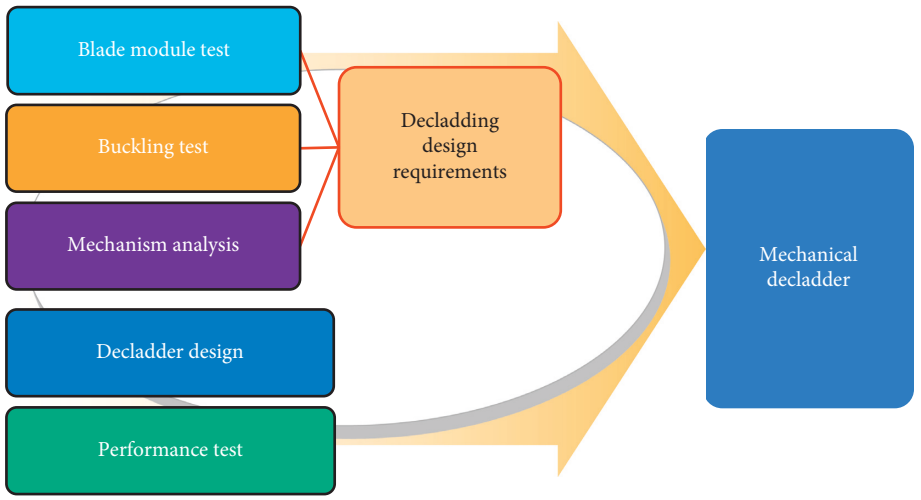

Figure 2: Design considerations.

As shown in Figure 3, a screw press-in part transfers force to a screw through a servomotor, and the load for the slitting force is applied at the bottom in the slitter. The slitting blade module installed at the bottom measures the slitting force when rods are penetrated and slit; standard trapezoid screws and nuts are used. The length of the part of the simulated rods and extrusion pin at the point where they pass through the slitting module and reach the bottom is set to a minimum of approximately 420 mm. A ball bush and a guide axis are installed on both ends for balance and for soft press-in without external interference. The bottom base plate contains a hole to fix the support axis and to set the 2-CUT blade module and 3-CUT blade module (Figure 4) [14]. A capacity of 100–1000 kg is selected for the load cell, and RSC 232 is embedded in the controller.

As shown in Figure 5, the roller gradient of the cutting module is changed to visually observe the slitting degree of the Zry-4 tube. The data measured in the load cell are obtained using RSC 232 communication. The gap in the cutting blade is measured during the slitting of Zry-4, and Ø 9.5 mm is used for the Zry-4 rods. The roller gradient is modified

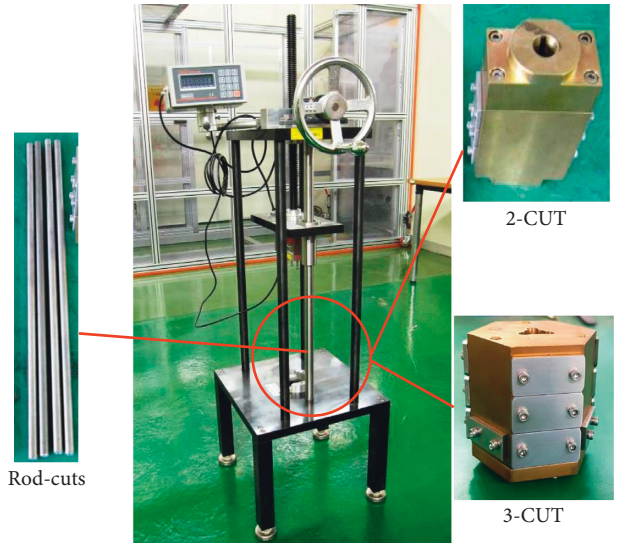

Figure 3: Slitter, 2-CUT and 3-CUT modules, and rod-cuts for slitting test.

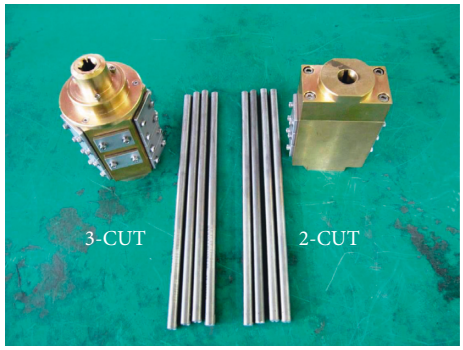

Figure 4: Blade types and simulated rod-cuts (2-CUT and 3-CUT modules).

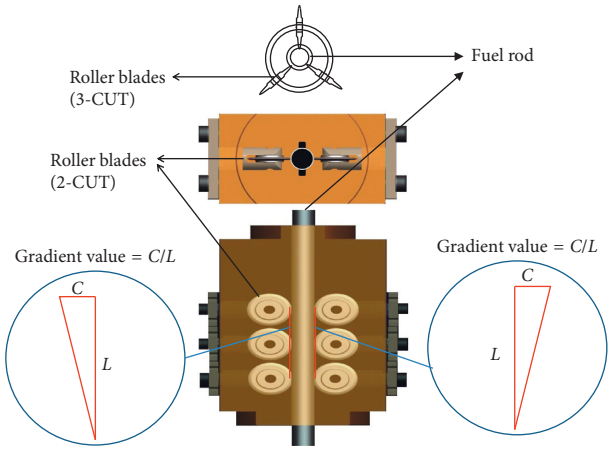

Figure 5: Roller gradient of 2-CUT and 3-CUT blade modules.

using an adjustment plate between blade jig and module, as shown in Figures 6(a) and 6(b). Aluminum pellets are inserted into a blank tube with a length of 250 mm for the testing to derive the optimal gradient value.

In the slitting for testing (Figure 3), cutting modules (Figure 4) were used to change the stepwise slitting velocity. The data measured in the load cell (BS-7220) were acquired using RSC 232 communication. Figure 7 shows the shape of the slit after the experiment using the 2-CUT and 3-CUT blade modules. Zry-4 rod-cuts (tube + Al pellets), 2-CUT blade module with a gradient of 200 (L/C), and 3-CUT blade module with a gradient of 133 (L/C) were used. As a result, the 2-CUT module did not slit both ends of the rod-cut, whereas the 3-CUT module slit the rod-cut completely.

For the design of the device, a measurement system was fabricated to test simulated rod-cuts and measure the slitting force. As shown in Figure 8, the maximum forces of the 2-CUT and 3-CUT blade modules at a velocity of 12.5 mm/s are 197.5 kgf and 363.2 kgf, respectively. At a velocity of 12.5 mm/s, The 2-CUT module requires less slitting force than the 3-CUT module. However, it cannot slit the tube, as shown in Figure 7, and it is unstable owing to two blades. Therefore, we selected the 3-CUT module.

2.4. Buckling Test. To obtain the requirements of the decladding mechanism, we used SolidWorks prosimulation to analyze the displacements of the empty Zry-4 tube under an extrusion force of 160 kgf for various lengths, specifically, 300 mm, 400 mm, 500 mm, and 600 mm. In the results, all fuel rod lengths (300, 400, 500, and 600 mm) were within the safe range without buckling. However, considering safety, we conservatively selected a fuel rod length of 500 mm.

The optimum decladding rod-cut length for buckling prevention was calculated. Figure 9 shows the results of the variation in displacement with length by SolidWorks prosimulation.

To verify the theoretical values shown in Figure 9, a buckling measurement instrument was used to perform a buckling verification test according to the length of the Zry-4 tube, as shown in Figure 10. Figure 11 shows similar trends as a result of synthesizing the theoretical and experimental values of displacements.

2.5. Mechanism Analysis. Based on the direction in which the fuel rod to be slit is placed, the mechanical decladder is categorized into the vertical, horizontal, and slant types [10]. As shown in Table 1, the advantages and disadvantages of the vertical, horizontal, and slant type decladding devices are compared and analyzed. It is required that the supply of rod-cuts should be continuous and that the durability of the blades should be maintained for a long time. As a result of the analysis of the general vertical, horizontal, and slant type decladders, the slip guide of the rod loading unit was set as inclined and the mechanism through which the rod-cut was supplied and slit was set as horizontal.

As shown in Table 2 and Figure 12, the hydraulic and electric drives were compared and analyzed in terms of slitting time, maintenance, and driving method. The dimensions ($L \times W \times H$, mm) of the electric type and hydraulic type are $1060 \times 800 \times 1060$ and $1410 \times 600 \times 1410$, respectively, as shown in Figure 12(a). Even though the hydraulic system has the disadvantage that stroke length is longer than that of the electric system for operation in a hot cell, the hydraulic system is preferred because of its low inertia, good momentary stoppage, easy maintenance, simplicity, and high slitting efficiency.

3. Results and Discussion

3.1. Mechanical Decladder Design. As shown in Table 3, the design requirements of the mechanical decladder were derived through preliminary testing and structural analysis. Based on experimental results and analytical data, the device was designed as a horizontal-type one.

We constructed the main mechanism designed using SolidWorks and fabricated the mechanical decladder based on the derived requirements. The mechanical decladder is shown in Figure 13.

As shown in Figure 13, the main mechanism consists of an autofeeding basket that continuously feeds rod-cuts, a hydraulic cylinder, a power unit to seat the rod-cuts, and a loading unit. In addition, it includes four-blade modules that separate the rod-cuts moved by the extrusion pin into hull pieces and pellets, a blade module housing that can be

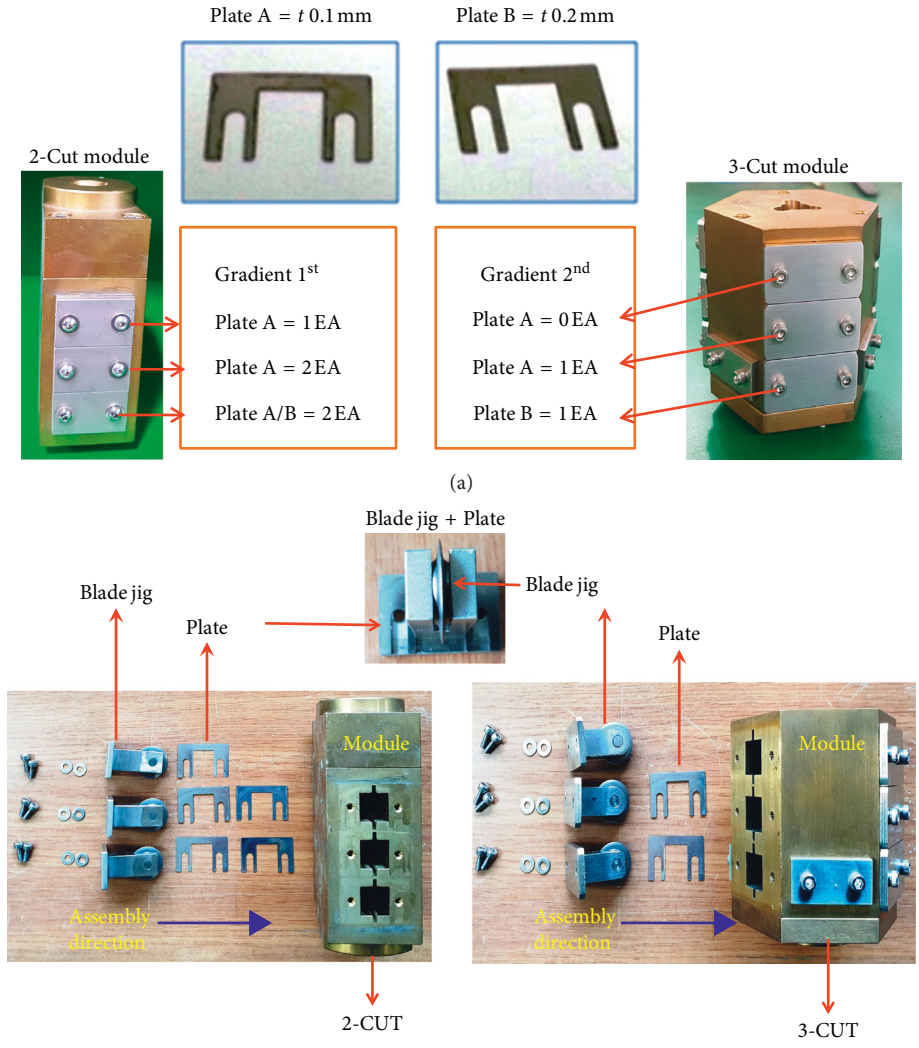

Figure 6: Gradient variable of modules using the plate: (a) assembly of module; (b) disassembly of module.

Figure 7: Slitting shapes of 2-CUT and 3-CUT modules.

rotated alternately with four-blade modules, and a basket to collect hulls and pellets [15, 16].

Figure 14(a) shows the main mechanism for decladding the rod-cuts. When the rod-cuts are filled into the autofeeding basket, the hydraulic cylinder is retracted and a pinion gear is rotated. Figure 14(b) shows the main module of the practical mechanical decladder. As the rod feeding unit and rod loading unit are mechanically connected, if the rod feeding unit moves forward and backward, the rod loading unit moves up and down simultaneously. In addition, the blade housing is fitted with four-blade modules at 90° (degree) intervals. When the blade housing is rotated, it is precisely aligned with the extrusion pin by fixing pins.

Figure 15 shows the rod-cut feeding mechanism that transfers rod-cuts from the autofeeding basket to the loading unit. While the hydraulic cylinder is retracting, rack gear A is retracted in the same direction as the hydraulic cylinder and pinion gears A and B are rotated simultaneously, as shown in Figure 15. Rack gear B is raised if pinion gear B is rotated. If rack gear B is raised, the rotation gear at the bottom of the autofeeding basket is rotated, the bottom of the autofeeding basket is opened, and the rod-cut falls onto the loading unit below.

Figure 16 shows the loading mechanism devised to alleviate the impact force when a rod-cut falls from the autofeeding basket onto the loading unit. If the impact of the rod-cut is large, the pellet fragments in the rod-cut will exit

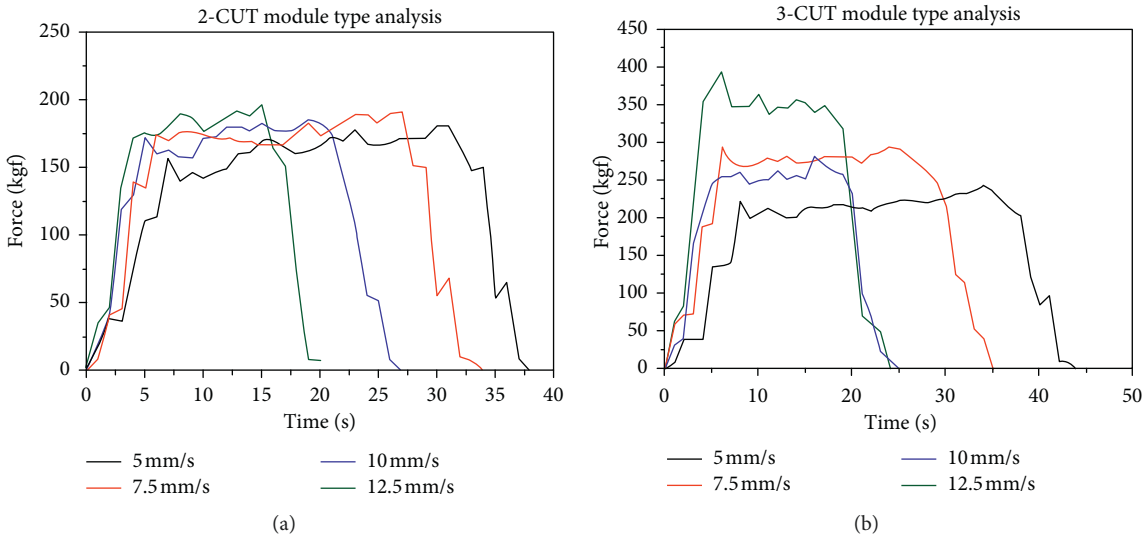

Figure 8: Variation in forces (kgf) on the 2-CUT and 3-CUT blade modules: (a) 2-CUT module; (b) 3-CUT module.

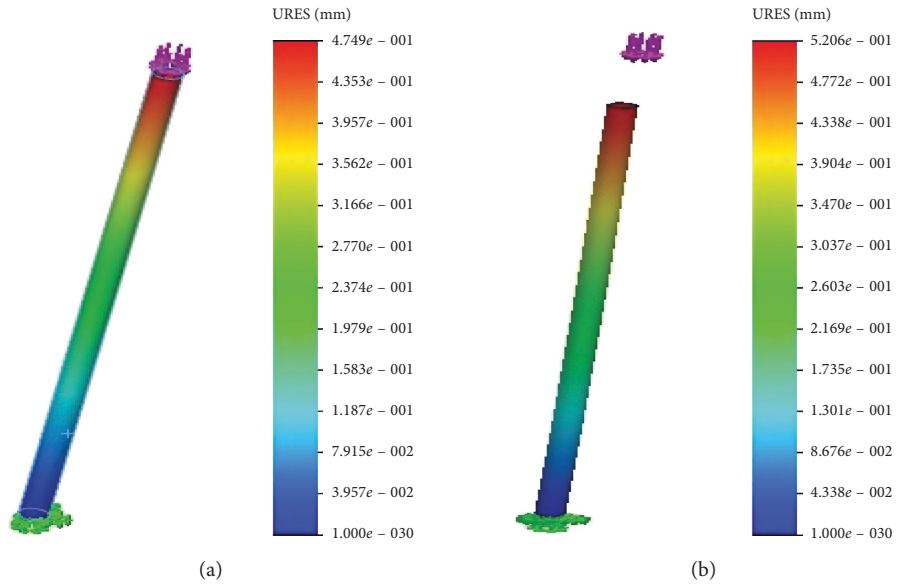

Figure 9: Continued.

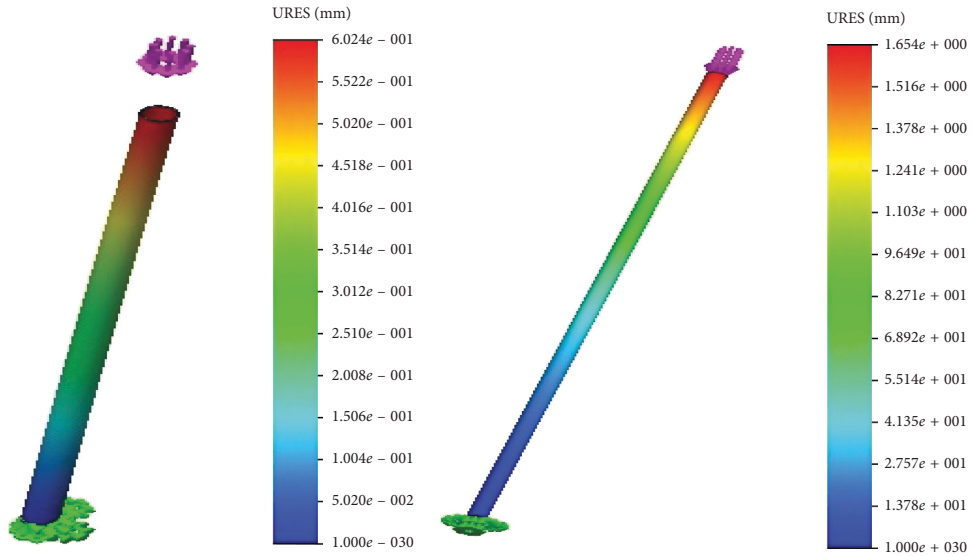

(c) (d)

Figure 9: Displacement according to Zry-4 tube lengths: (a) 300 mm, (b) 400 mm, (c) 500 mm, and (d) 600 mm.

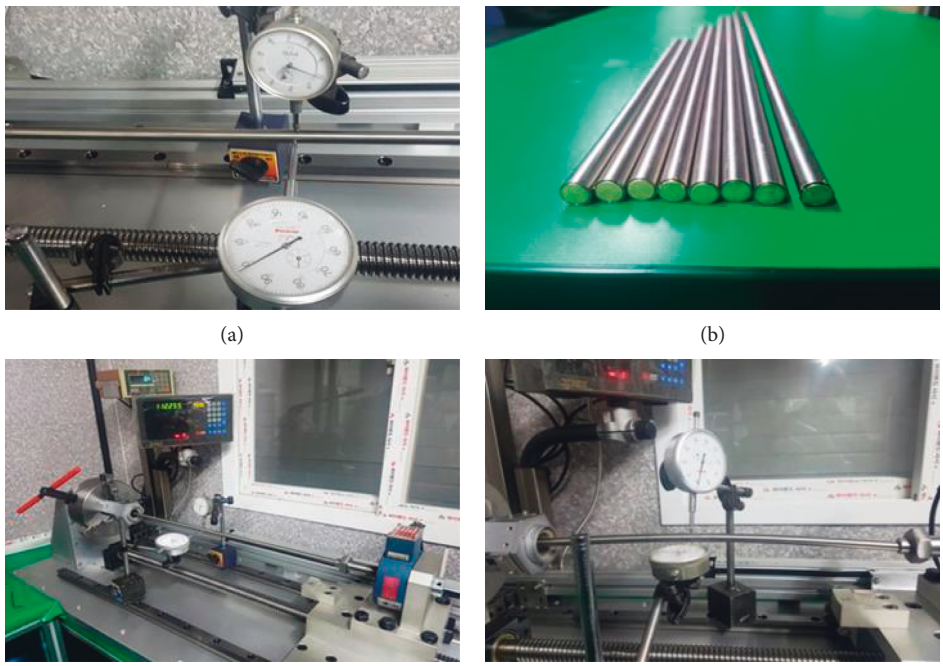

(a) (b)

(c) (d)

Figure 10: Buckling test according to Zry-4 tube lengths: (a) rod-cuts, (b) instrument, (c) measurement, and (d) buckling.

the rod-cut and the mechanism will be contaminated. A loading unit is kinematically devised to prevent this. The principle of the loading mechanism is as follows: As shown in Figure 16, if the point A moves backward and descends according to the slope of point B, the loading unit is raised by spring tension. At this time, the impact force of the rod-cut falling from the autofeeding basket decreases, owing to the short fall height. In addition, if the rod-cut lands on the loading unit, the extrusion pin is moved to the blade module while applying force to the rod-cut via hydraulic pressure.

The rotation of the blade module housing enables the durability of the blade to be maintained for a long time because the overheating of the blade is prevented [17, 18]. As shown in Figure 17, four-blade modules are mounted around the housing axis. Two pairs of facing blade modules simultaneously slit rod-cuts, and after a certain period, the

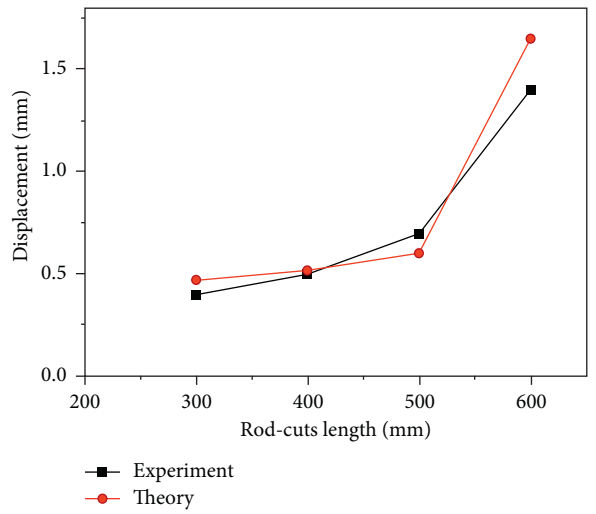

Figure 11: Comparison of experimental and theoretical displacements of the Zry-4 tube.

Table 1: Advantages and disadvantages of different types of decladders.

Content	Advantage and disadvantage	Type		
		Vertical	Horizontal	Slant
Design/ fabrication	Advantage		Easy rod-cut feeding	Easy to remove fragments after decladding
	Disadvantage	(i) UO_2 fragments emitted before decladding (ii) Difficult rod-cut feeding	Fragments remain in blade after decladding	Difficult rod-cut feeding
Working process	Advantage	(i) Simple (ii) Low blade wear	(i) Simple (ii) Low blade wear	
	Disadvantage			(i) Complicated (ii) High blade wear
Efficiency	Advantage		High	High
	Disadvantage	Low		

Table 2: Comparison of electric and hydraulic types for selection.

Type	Electric	Hydraulic
1	*No oil leakage*	Oil leakage occurs
2	*No pressure loss*	Pressure loss occurs
3	Low efficiency	*High efficiency*
4	Difficult to maintain	*Easy to maintain*
5	*No fraction and lubrication required*	Fraction and lubrication required
6	High inertia	*Low inertia (momentary stop and run)*
7	Complexity	*Simplicity*
8	*Short stroke*	Long stroke

other two blade modules are alternated for the next decladding operation. When the blade module housing is rotated to 90°, the alignment pin on the side of the module housing locks the housing using a spring.

The side-view schematic of the 3-CUT blade module is shown with the housing removed to illustrate the configuration of the module (Figure 18). Each row of slitting blades is indexed from the center of the assembly to progressively cut into tubing. Slitting blades are arranged at 120° intervals around the center of the 3-CUT blade module, as shown Figure 18. Upon exiting a rod-cut, hulls and pellets are collected directly below the assembly.

3.2. New Mechanical Decladder. As shown in Figures 19 and 20, the mechanical decladder is manufactured based on the mechanism requirements and design. In a mechanical decladder, a decladding assembly as a unit for rod-cuts includes slitting blades for decladding and rollers for guiding the extrusion of cladding tubes. The slitting blades and

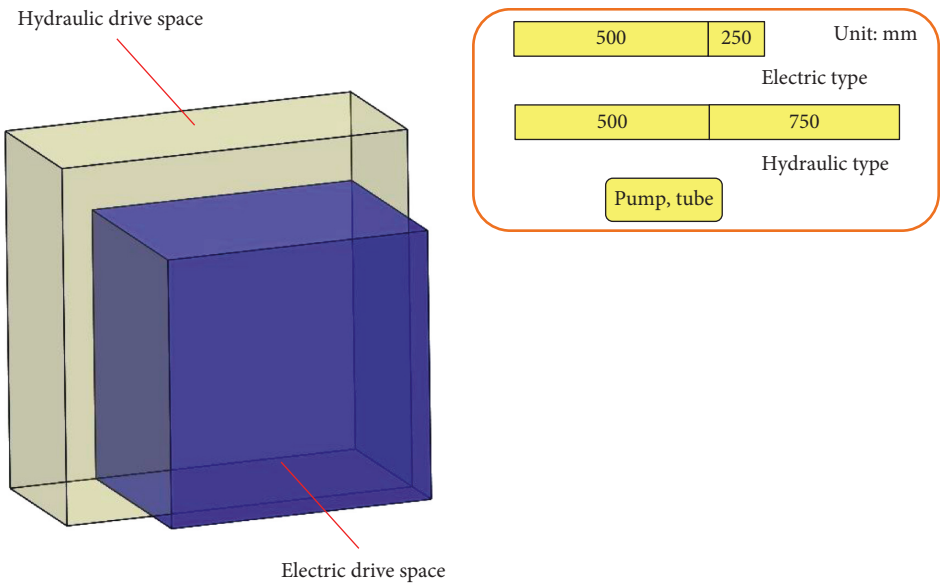

Figure 12: Comparison of electric and hydraulic type for space: (a) space; (b) length.

Table 3: Design requirements of mechanical decladder.

Contents	Design requirements	Remarks
Capacities	(i) 4 m fuel rod/4 min (1 rod-cut/30 s) (ii) Process time of PWR 16 × 16 assembly: 15 h × 2 units (iii) Rod-cut: 500 mm length	PWR (pressurized water reactor)
Extrusion method	(i) Cylinder drive: hydraulics (ii) Cylinder quantity: double acting × 2 units	AC 220 V, 3 P
Blade	(i) Blade material: high-speed steel (ii) Blade module quantity: 4 modules (iii) Blade type: 3-CUT blade modules	
Feeding and recovery	(i) Horizontal type (ii) Rod-cut feeding: rack and pinion, autofeeding (iii) Separation of hulls and fragments	37.5 kg HM-U/batch: 1 unit

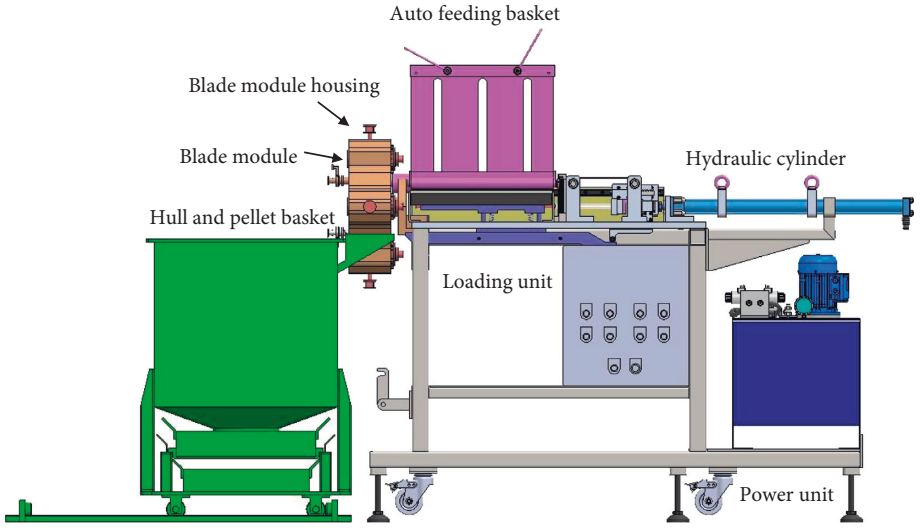

Figure 13: Main mechanism of mechanical decladder.

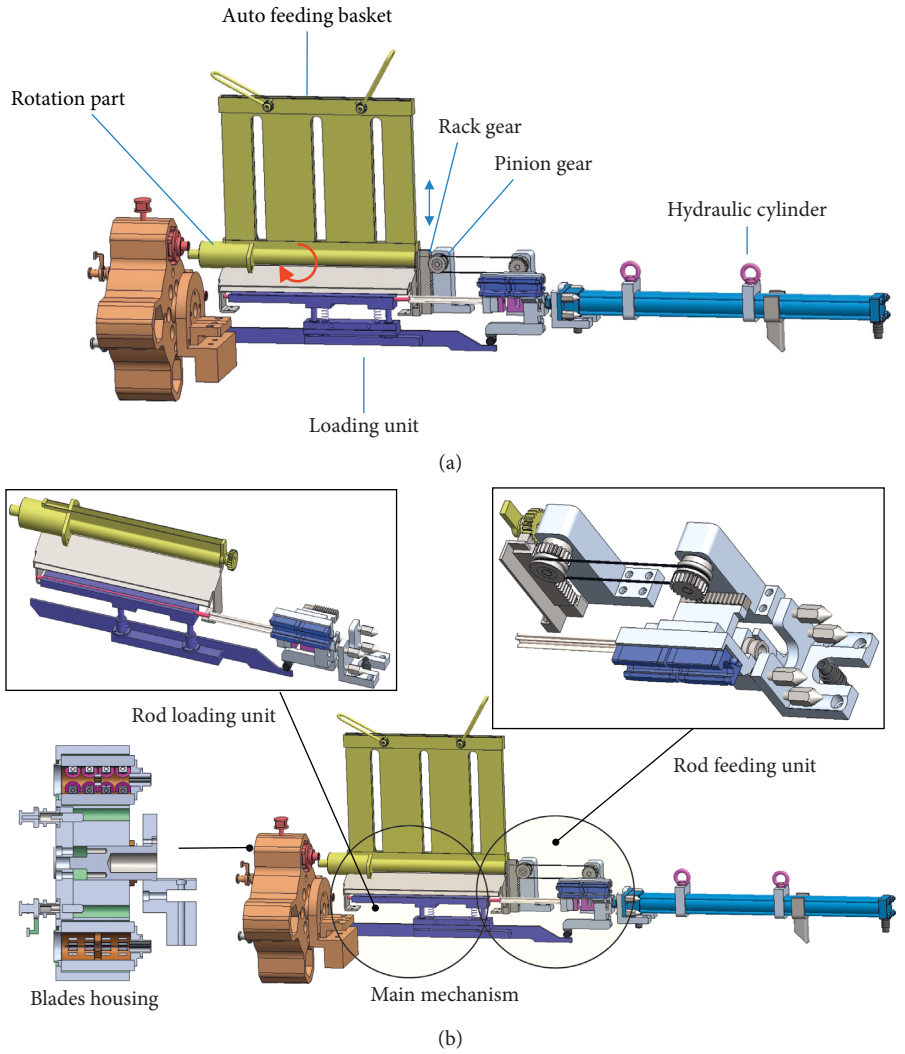

Figure 14: Main modules of practical scale mechanical decladder: (a) mechanism; (b) main modules.

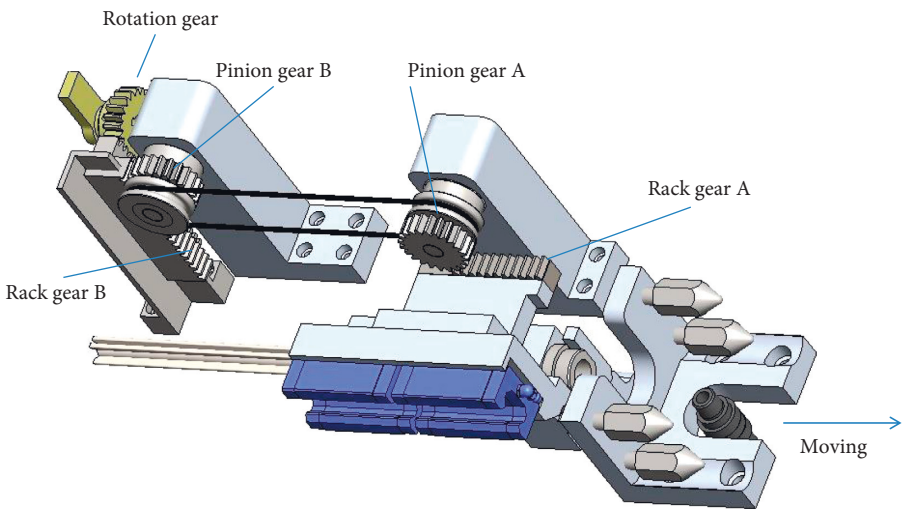

Figure 15: Rod-cut feeding mechanism.

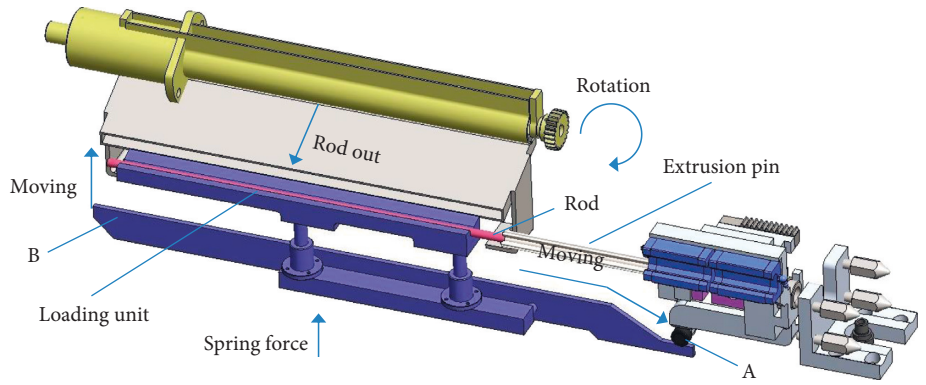

Figure 16: Rod-cut loading mechanism.

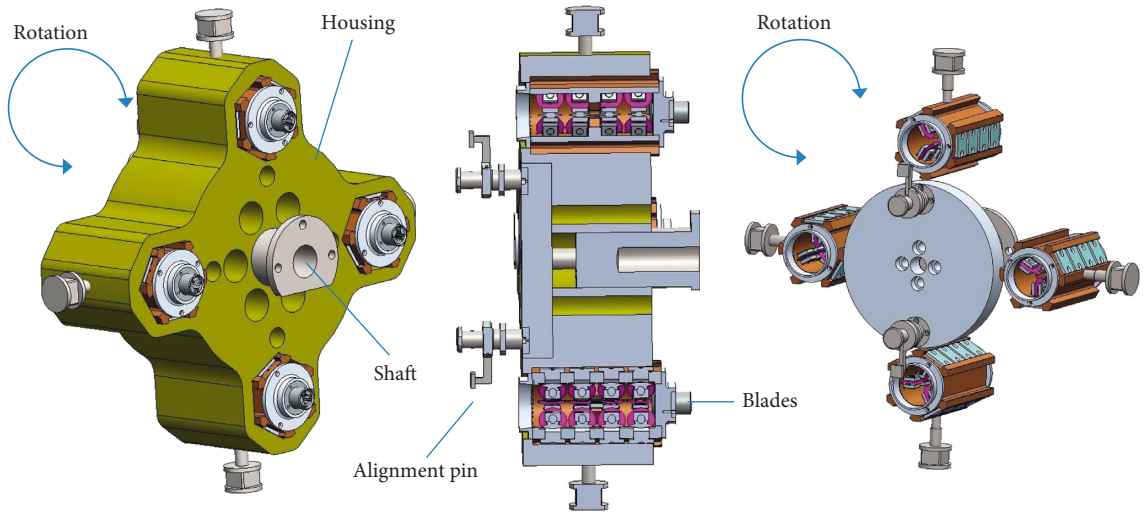

Figure 17: Blade module housing.

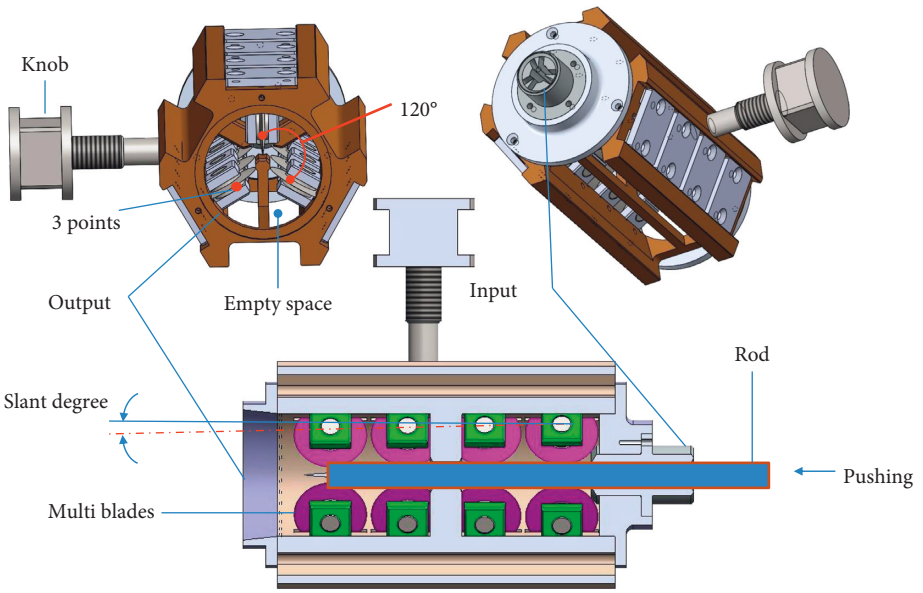

Figure 18: Schematic of 3-CUT blade module.

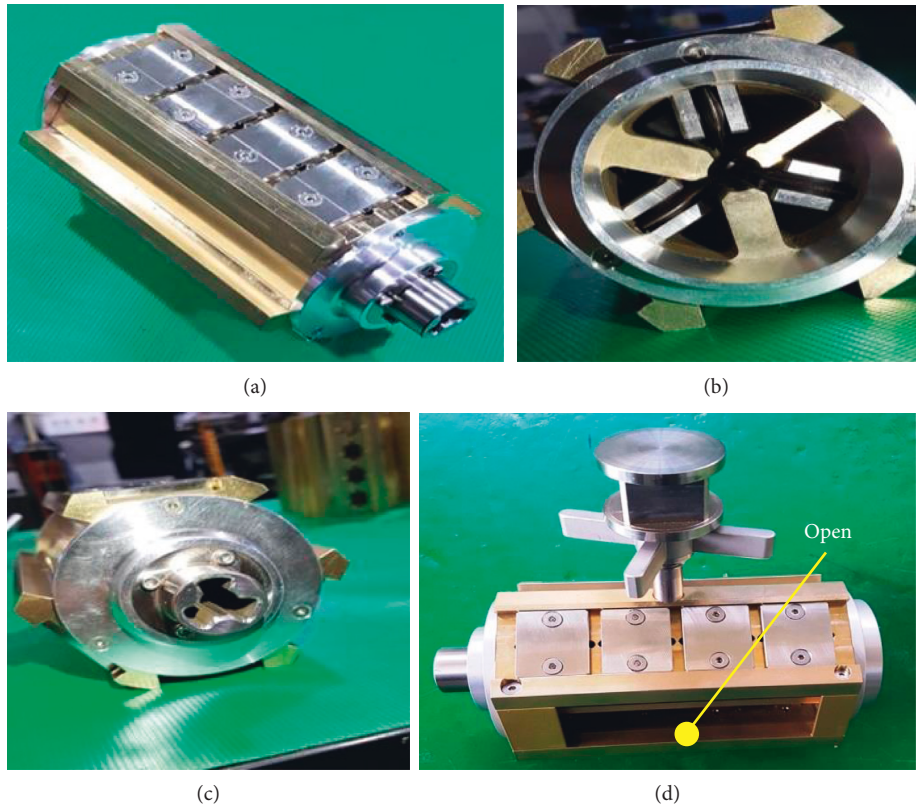

Figure 19: Newly developed 3-CUT blade module and loading unit: (a) front view, (b) left view, (c) right view, and (d) loading unit.

rollers of the decladding assembly are configured such that the rollers are placed between the respective neighboring slitting blades at intervals of approximately 120° in the circumferential direction, as shown in Figure 19(b). The slitting intervals of rod-cuts with different diameters are controlled by adding or removing a spacing plate between a slitting blade and a ranch bolt for fixing the slitting blade to the slitting assembly, as shown in Figure 19(a). The mechanical decladder can be applied to fuel rods of various lengths, including cladding tubes of various thicknesses, if modules of various sizes are utilized. In addition, the mechanical decladder provides a mechanism capable of slitting fuel rods of various diameters. The horizontal-type mechanical decladder includes multiple rollers configured to receive, extrude, and transfer a rod-cut. The slitting portion is placed at the end of the rollers, and the distance between a guide bar and a blade roller in the roller fixing portion is reduced in the direction toward the slitting portion. The decladding of rod-cuts is performed by the rotation of three circular cutting blades inserted among the rollers arranged at 120° intervals. The rollers receive and transfer fuel rods into the entrance using the extrusion pin, as shown in Figure 19(c). Specifically, a roller arranged at the first end receives a rod-cut whose upper and lower caps are removed. The extrusion velocity with respect to the fuel rods is controlled by the hydraulic pressure applied to the fuel rods. Such an operation is controlled by the pressure of a hydraulic cylinder placed at the rollers. Moreover, when the 3-CUT blade module slits the rod-cut horizontally, some fragments accumulate on the blade rotation shaft inside the 3-CUT blade module. To prevent this, one side of the 3-CUT blade module was opened horizontally, as shown in Figure 19(d). The 3-CUT blade module separates the spent UO_2 pellet from the clad tube by passing the rod-cut through four sets of cutter blades [19]. Each set comprises three cutters distanced from each other at 120° and the distance between the centers of the blades decreased gradually. Thus, it has a longer blade life owing to less frictional force.

Figure 20 gives a practical view of the practical scale mechanical decladder. The size of the device is $3000 \times 1200 \times 1500$ mm ($L \times W \times H$). The entire configuration consists of an autofeeding basket module that continuously feeds rod-cuts, a hydraulic cylinder module, a power unit module, and a loading unit module, which seats and presses rod-cuts. Additionally, it includes a blade module that separates a rod-cut advanced by the extrusion pin into a hull piece and a pellet piece, a blade module housing that can be rotated alternately using four-blade modules, a hulls and pellets basket module, another feeding system module, a control panel module, and a supporter module. The material is mainly stainless steel, and the blade module housing is created using light aluminum in consideration of the maintenance of remote operation. In addition, a load cell is installed between the hydraulic cylinder and extrusion pin to measure cutting force and cutting velocity. A data acquisition system capable of obtaining data using RSC 232 is

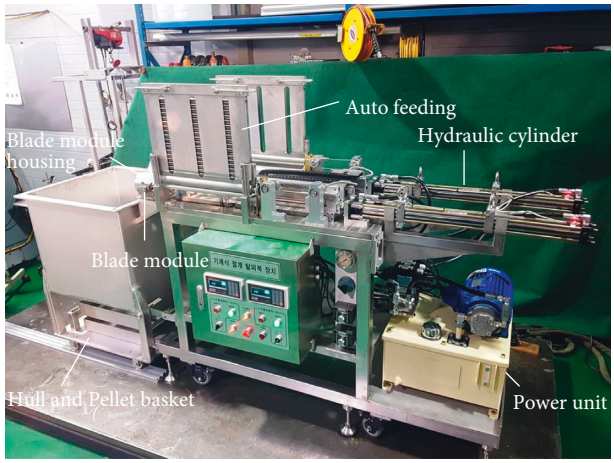

Figure 20: Practical scale mechanical decladder.

constructed. The control panel can control the forward and backward movement of the extrusion pin, hydraulic flow rate, and hydraulic velocity.

3.3. Basic Performance Test. As shown in Figure 21, 37.5 kg of uranium HM/batch is loaded into the autofeeding basket of the mechanical decladder. This corresponds to 156 pieces with a rod-cut length of 500 mm. When the autofeeding basket is pulled up by a crane and a master slave manipulator, the hydraulic cylinder at the back moves backward and the loading unit rises. At the same time, one rod-cut in the fuel rod basket is seated in the loading unit. At this time, as the hydraulic cylinder advances, the extrusion pin advances while pushing the seated rod-cut. The load cell measures slitting force and transmits it to the data acquisition device. When the extrusion pin passes through the blade module, hulls and pellets are separated and placed in the bottom basket. Then, the hulls and the pellets are placed in a container and sent to the voloxidation process.

The decladding efficiencies obtained by slitting the fuel rod-cuts with various burnups of used PWR nuclear fuels discharged from domestic commercial nuclear power plants in Korea [20]. Above a burnup of 40 GWd/tU, the used fuel with a rim structure was generally categorized as a high-burnup fuel [21, 22]. The decladding efficiency by slitting fuel rod-cuts was observed to be fully dependent on the pellet-cladding gap characteristics with fuel burnup. The gap between the pellets and cladding during irradiation was completely closed around a burnup of 30 GWd/tU [23]. However, the pellet-cladding gap reopens when there is a difference in thermal expansion between the pellet and the cladding during the cooling-down step [24]. As fuel burnup increases, the mean width of the pellet-cladding gap decreases and then becomes zero when there is a burnup that is approximately above 50 GWd/tU [25]. The decladding efficiency shows a significant difference with burnups below and above 40 GWd/tU [26]. This difference is attributed to a decrease in the pellet-cladding gap width with an increase in the fuel burnup [25]. This is confirmed by a visual observation of fuel material that adheres to the inner walls of split claddings. In addition, most claddings were split into three pieces. Even though some claddings were split into two pieces, the fuel fragments were successfully recovered [20]. If there are fuel fragments in the inner walls of split claddings, it is oxidized in the oxidative decladding process.

Simulated rod-cuts (Zry-4 tube + brass pellets) were fabricated for slitting. The zircaloy tube (PWR 16 × 16) was 10.7 mm in outer diameter, 9.5 mm in inner diameter, and 0.65 mm in thickness, and the pellet was 9.4 mm in outer diameter and 10 mm in length. There were 50 simulated pellets in the zircaloy tube with a length of 500 mm. The material of the pellets was selected as brass, considering UO_2 pellet hardness and blade abrasion on the ceramic. Figure 22 shows the simulated rod-cuts. The clearance gap between the Zry-4 tube and brass pellets is 0.5 mm. Brass pellets were used for the continuous slitting of the PRIDE mechanical decladder in place of real PWR spent UO_2 pellets in conservative conditions, as the compressive fracture stress of the brass pellets was higher than that of real PWR spent UO_2 pellets.

Figure 23 shows the mechanical decladder with a simulated rod-cut element and the experimental setup of the cutting wheel assembly. A simulated rod-cut was prepared for preliminary testing of the decladding device, and a data acquisition system was constructed using RSC 232 to measure the decladding force and velocity [27].

The mechanical decladder slit a rod-cut as follows: When a simulated rod-cut of spent nuclear fuel was placed at the blade module entrance, it was inserted into the center of the module by the extrusion pin. Subsequently, the rod-cut passed through the module, where it was separated into several pieces by blades, and hulls and pellets were recovered simultaneously.

Figure 23 shows the main setup of the rod-cut slitting test. As shown in Figure 23(a), when the rod-cut is seated, it is pressed in while the extrusion pin at the rear advances, as shown in Figure 23(b). The rod-cut pressed into the blade module is discharged through four-stage blades, as shown in Figure 23(c). As shown in Figures 23(d)–23(f), the rod-cut passes through the blade module and is cut into three pieces, which are collected by gravity [28]. When the simulated rod-cuts (Zry-4 tubes + brass pellets) were used, the housing module of the mechanical decladder could maintain the durability of the blade, the measured slitting force was 326 kgf (Figure 24), and cutting velocity was 16.7 mm/s. Moreover, as the section of the Zry-4 tubing was fitted with solid brass pellets for internal support during passage through the 3-CUT blade module, the rod-cut was completely sectioned in three evenly spaced locations.

4. Conclusions

KAERI is developing a pyroprocess. As a part of the process equipment, a practical scale mechanical decladder that can slit spent nuclear fuel rod-cuts (hulls + pellets) of several tens kg HM/batch is being developed to supply UO_2 pellets to a voloxidation process. The engineering design of the mechanical decladder consisted of five parts; specifically, blade module test, buckling test, mechanism analysis, decladder

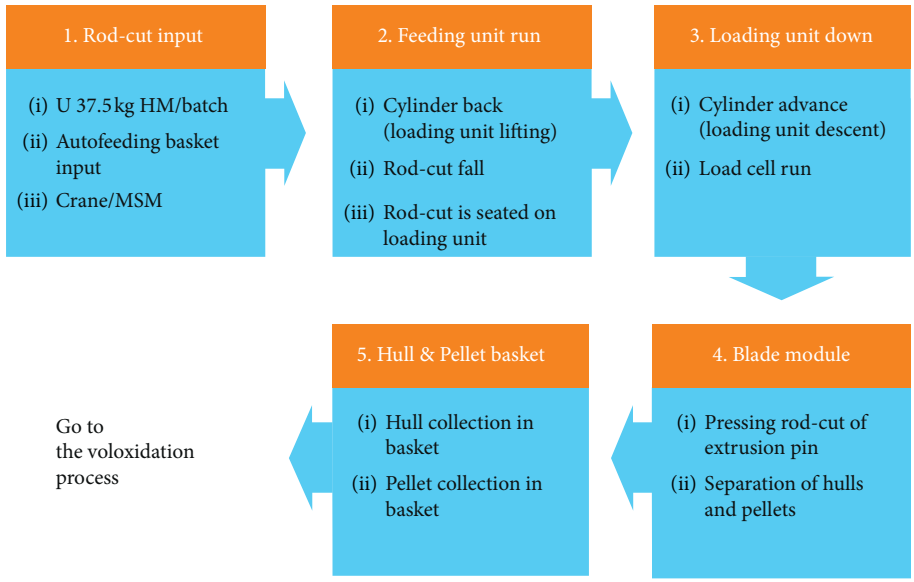

Figure 21: Operating procedure of mechanical decladder.

Figure 22: Simulated rod-cuts (length: 500 mm).

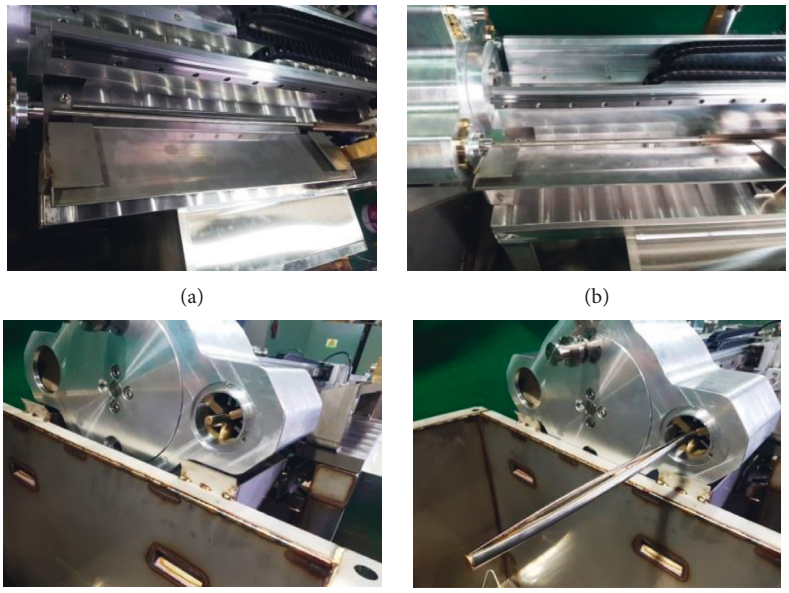

(a) (b) (c) (d)

Figure 23: Continued.

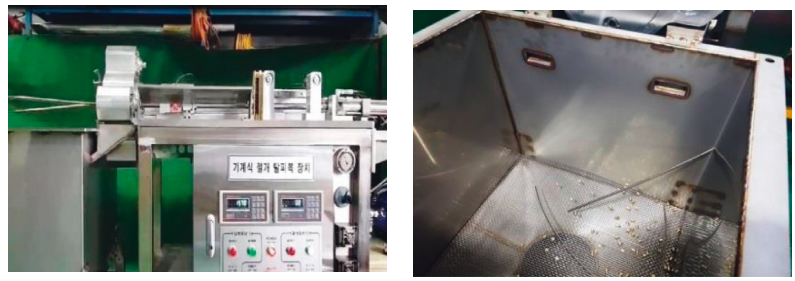

(e) (f)

Figure 23: Mechanical decladding test of rod-cut: (a) seating, (b) extrusion, (c) discharge, (d) decladding, (e) falling, and (f) collection.

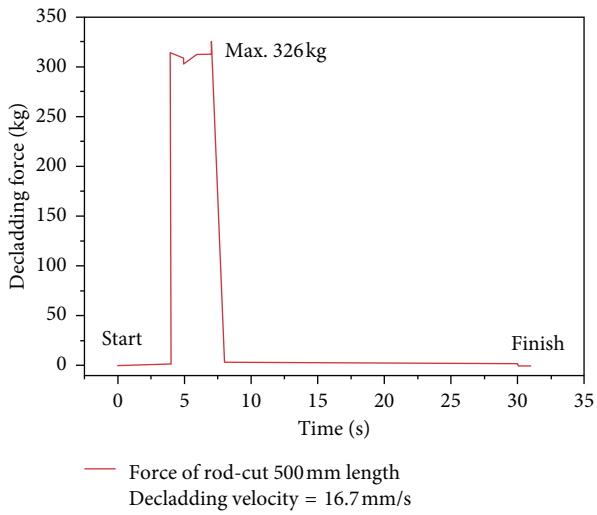

Figure 24: Slitting force and velocity of rod-cut.

design, and basic performance test. Blade module pretesting was conducted using a prototype device to obtain design requirements. The 2-CUT module did not slit both ends of a rod-cut, whereas the 3-CUT module slit them completely. Even though the 2-CUT module exhibited less resistive force than the 3-CUT module, it could not slit the rod-cuts and was unstable owing to it having two blades. Hence, the 3-CUT module was selected for the mechanical decladder. To obtain the requirements of the decladding mechanism, we used SolidWorks prosimulation to analyze the displacement of the rod-cuts, with lengths of 300 mm, 400 mm, 500 mm, and 600 mm when the extrusion force on the tube was 160 kgf. Furthermore, to verify the theoretical value of buckling stress, a buckling measurement instrument was used to perform a buckling verification test according to the length of each rod-cut. Rod-cut displacements according to lengths showed similar trends as a result of synthesizing the theoretical and experimental trends of variation in rod-cut displacement with length. A rod-cut with a length of 600 mm did not exceed yield stress. However, there was a problem in safety design because of bending. Therefore, when using a rod-cut length of 600 mm, a support should be designed with two points on the feeding module to prevent buckling during decladding. All fuel rod lengths (below 500 mm) were within the safe range without buckling. For the analysis of the decladding mechanism, the vertical, horizontal, and slant type mechanical decladders were considered, according to the direction in which the fuel rod to be slit was placed. As a result of the analysis, the orientation of the mechanism through which the rod-cut was supplied and slit was selected as horizontal. The hydraulic and electric drives were analyzed in terms of slitting, maintenance, and driving method. The hydraulic system was preferred because of its low inertia, good momentary stoppage, easy maintenance, and high slitting efficiency. The design requirements of the mechanical decladder were derived through preliminary testing and structural analysis. The horizontal-type decladder was selected based on experimental results and analytical data. In this type of decladder, the main mechanism consisted of an autofeeding basket that continuously fed rod-cuts, a hydraulic cylinder, a power unit to seat the rod-cuts, and a loading unit. It also included four-blade modules that separated the rod-cuts moved by the extrusion pin into hull pieces and pellets, a blade module housing that could be rotated alternately with four-blade modules, and a basket to collect hulls and pellets.

The mechanical decladder was manufactured based on the mechanism requirements and design. By utilizing the new mechanical decladder, the slitting intervals of rod-cuts with different diameters were controlled by adding or removing a spacing plate between a slitting blade and a ranch bolt for fixing the slitting blade to the 3-CUT module. The practical scale mechanical decladder can be applied to fuel rods of various lengths, including cladding tubes of various thicknesses, if blade modules of various sizes are used.

Rod-cuts (Zry-4 tube + brass pellets) were fabricated for decladding. There were 50 simulated pellets in a zircaloy tube with a length of 500 mm. The material of the pellets was selected as brass considering UO_2 pellet hardness and blade abrasion. In the decladding results obtained using the rod-cuts, the housing module of the mechanical decladder maintained the durability of the blades for a long period, decladding force was 326 kgf, and cutting velocity was 16.7 mm/s. Additionally, the tubing was completely sectioned into three evenly spaced locations. Consequently, the design process for the mechanical decladder can contribute to the optimum design of a compact mechanical decladder with high efficiency in a hot cell, and it will be utilized in the design of a more efficient mechanical decladder in the future.

Data Availability

The data used to support the findings of this study are available from the corresponding author upon request.

Conflicts of Interest

The authors declare that they have no conflicts of interest regarding the publication of this paper.

Acknowledgments

This work was supported by the National Research Foundation of Korea (NRF) grant funded by the Korean government (MEST) (no. 2012M2A8A5025696).

References

[1] J.-H. Yoo, C.-S. Seo, E.-H. Kim, and H.-S. Lee, "A conceptual study of pyroprocessing for recovering actinides from spent oxide fuels," *Nuclear Engineering and Technology*, vol. 40, no. 7, pp. 581–592, 2008.

[2] K.-C. Song, H.-S. Lee, J.-M. Hur, J.-G. Kim, D.-H. Ahn, and Y.-Z. Cho, "Status of pyroprocessing technology development in Korea," *Nuclear Engineering and Technology*, vol. 42, no. 2, pp. 131–144, 2010.

[3] Y.-H. Kim, Y.-Z. Cho, J.-W. Lee, J.-H. Lee, S.-C. Jeon, and D.-H. Ahn, "Engineering design of a voloxidizer with a double reactor for the hull separation of spent nuclear fuel rods," *Science and Technology of Nuclear Installations*, vol. 2017, Article ID 9854830, 12 pages, 2017.

[4] G. Uchiyama, K. Yamazaki, S. Sugikawa, M. Maeda, T. Tsujino, and M. Kitamur, "Development of voloxidation process for tritium control in reprocessing," *Japan Atomic Energy Research Institute-M*, vol. 23, no. 11, pp. 91–199, 1991.

[5] F. H. Hammad, H. R. Higgy, and A. A. Abdel-Rassoul, "Mechanical decladding of nuclear fuel elements," *Journal of the British Nuclear Energy Society*, vol. 10, no. 1, pp. 21–28, 1971.

[6] H. Lee, G.-I. Park, J.-W. Lee et al., "Current status of pyroprocessing development at KAERI," *Science and Technology of Nuclear Installations*, vol. 2013, Article ID 343492, 11 pages, 2013.

[7] Y. H. Kim, H. J. Lee, J. K. Lee et al., "Engineering design of a high-capacity vol-oxidizer for handling UO_2 pellets of tens of kilogram," *Journal of Nuclear Science and Technology*, vol. 45, no. 7, pp. 617–624, 2008.

[8] G. Uchiyama, S. Torikai, M. Kitamura et al., "Outline of an experimental apparatus for the study on the advanced voloxidation process," *Japan Atomic Energy Research Institute-M*, vol. 21, no. 1, p. 90, 1990.

[9] W. Stumpf, H. Queiser, R. Kuhnel, G. Zeitzschel, and G. Dannehl, "Process and device for reprocessing nuclear fuels," European Patent No. EP0039815A1, 1981.

[10] J. H. Jung, J. S. Yoon, Y. H. Kim, J. H. Jin, and D. H. Hong, "Separation and receiving device for spent nuclear fuel," US Patent 7,673,544 B2, 2010.

[11] M. F. Simpson, "Projected salt waste production from a commercial pyroprocessing facility," *Science and Technology of Nuclear Installations*, vol. 2013, Article ID 945858, 8 pages, 2013.

[12] H.-S. Lee, G.-I. Park, K.-H. Kang et al., "Pyroprocessing technology development at KAERI," *Nuclear Engineering and Technology*, vol. 43, no. 4, pp. 317–328, 2011.

[13] J. S. Yoon, S. H. Kim, and T. G. song, "Analysis of remote operation involved in spent nuclear fuel conditioning process using its virtual mockup," in *Proceedings of the International Conference on Control, Automation, and System (ICCAS2004)*, pp. 840–845, The Shangri-La Hotel, Bangkok, Thailand, August 2004.

[14] R. Duncan and F. CelliOe, "Nuclear reactor fuel rod splitter," US Patent 3,831,248, 1974.

[15] W. Yan and B. O. Nnaji, "Functionality-based modular design for mechanical product customization over the internet," *Journal of Design and Manufacturing Automation*, vol. 1, no. 1-2, pp. 107–121, 2001.

[16] C.-C. Huang, "Overview of modular product development," *Proceedings of the National Science Council, Republic of China (A)*, vol. 24, no. 3, pp. 149–165, 2000.

[17] Y.-T. Tsai and K.-S. Wang, "The development of modular-based design in considering technology complexity," *European Journal of Operational Research*, vol. 119, no. 3, pp. 692–703, 1999.

[18] D. W. He and A. Kusiak, "Design of assembly systems for modular products," *IEEE Transactions on Robotics and Automation*, vol. 13, no. 5, pp. 646–655, 1997.

[19] K. Okada, "Separation method for a spent fuel rod," European Patent Application No. 19850302514, 1985.

[20] J.-W. Lee, D.-Y. Lee, Y.-S. Lee et al., "Estimation on feeding portions of slitting decladded fuel fragments to electrolytic reduction process," *Nuclear Technology*, vol. 204, no. 1, pp. 101–109, 2018.

[21] H. Stehle, "Performance of oxide nuclear fuel in water-cooled power reactors," *Journal of Nuclear Materials*, vol. 153, pp. 3–15, 1988.

[22] H. Matzke, H. Blank, M. Coquerelle et al., "Oxide fuel transients," *Journal of Nuclear Materials*, vol. 166, no. 1-2, pp. 165–178, 1989.

[23] J. L. Guillet and Y. Guerin, *Nuclear Fuels*, CEA Saclay and Groupe Moniteur, Paris, France, 2016, http://www.materials.cea.fr/en/PDF/MonographiesDEN/Nuclearfuels-CEA-en.pdf.

[24] K. Tanaka, K. Maeda, S. Sasaki, Y. Ikusawa, and T. Abe, "Fuel-cladding chemical interaction in MOX fuel rods irradiated to high burnup in an advanced thermal reactor," *Journal of Nuclear Materials*, vol. 357, no. 1–3, pp. 58–68, 2006.

[25] L. Desgranges, "Internal corrosion layer in PWR fuel," *Thermal Performance of High Burn-Up LWR Fuel*, p. 187, Organisation for Economic Co-operation and Development/Nuclear Energy Agency, Cadarache, France, 1998.

[26] J. A. King, T. J. Malewitz, S. M. James, and B. D. Simmons, "Mechanical decladding of irradiated FFTF mixed oxide fuel rods," *Transactions of the American Nuclear Society*, vol. 117, 333 pages, 2017.

[27] L. Steffensen, O. Than, and S. Büttgenbach, "BICEPS: a modular environment for the design of micromachined silicon devices," *Sensors and Actuators A: Physical*, vol. 79, no. 1, pp. 76–81, 2000.

[28] K. H. Kang, C. H. Lee, M. K. Jeon, S. Y. Han, G. I. Park, and S.-M. Hwang, "Characterization of cladding hull wastes from used nuclear fuels," *Archives of Metallurgy and Materials*, vol. 60, no. 2, pp. 1199–1203, 2015.